

CRS-stack-based seismic imaging workflow—theory and synthetic data example

T. Hertweck, J. Mann, E. Duvenceck, and C. Jäger

email: Thomas.Hertweck@gpi.uka.de

keywords: CRS stack, wavefield attributes, inversion, time migration, depth migration

ABSTRACT

The Common-Reflection-Surface stack method is a generalized multi-dimensional and multi-parameter stacking velocity analysis tool. In its application, emphasis has so far mainly been put on its ability to produce simulated zero-offset sections of high S/N ratio. However, the method also yields a number of so-called kinematic wavefield attributes. Based on these attributes, an entire seismic reflection imaging workflow can be defined that includes the Common-Reflection-Surface stack itself, an automated time migration, and the use of the wavefield attributes to determine a velocity model for depth migration. This imaging workflow is demonstrated on a synthetic 2D data example, starting from the preprocessed multicoverage data and leading to the final depth image.

INTRODUCTION

Seismic reflection data processing aims at obtaining the best possible image of the subsurface, either in the time or in the depth domain. Especially in regions with complex geological structures or for data with low signal-to-noise (S/N) ratio, this is a demanding task that usually requires extensive time-consuming human interaction. One possible alternative is to automatically extract as much information as possible directly from the measured data. The continuous advances in computing facilities make such data-driven approaches (e. g., Hubral, 1999) feasible which, thus, have increasingly gained in relevance in recent years. In this contribution, we focus on one of these methods, the Common-Reflection-Surface (CRS) stack (e. g., Müller, 1999; Jäger et al., 2001; Mann, 2002), and its integration into a processing workflow as is shown in a simplified way in Figure 1. This approach has already been introduced during the WIT meeting 2003 in Hamburg and is now elaborated in more detail.

The CRS stack provides a simulated zero-offset (ZO) section of high S/N ratio and is, thus, an alternative for the conventional NMO/DMO/stack approach (e. g., Yilmaz, 2001). Besides the improved ZO simulation, there is an additional benefit that is obtained with the CRS stack: instead of the usual stacking velocity v_{stack} , the process yields an entire set of so-called kinematic wavefield attributes. This additional information is very useful in further processing. Firstly, the CRS stack method allows to obtain a time-migrated section in an automated way. Secondly, the attributes can be utilized in a tomographic inversion (e. g., Duvenceck and Hubral, 2002; Duvenceck, 2004) which allows to obtain a velocity model for depth imaging. This establishes the link between the time and the depth domain. In contrast to conventional inversion approaches, this method does not assume continuous reflection events in the data and requires only minimum picking effort. It is well known that the quality of the (initial) macrovelocity model is crucial to successful depth imaging; the closer the model to the true effective velocity in the subsurface, the shorter the turn-around time. Finally, properties like, e. g., the geometrical spreading factor (Vieth, 2001) or the size of the projected Fresnel zone (Mann, 2002) can be estimated by means of the kinematic wavefield attributes. In principle, they can also be utilized in combination with the determined velocity model and the simulated ZO section in the Kirchhoff migration process itself to determine an optimal migration aperture. However, this application has not yet been implemented.

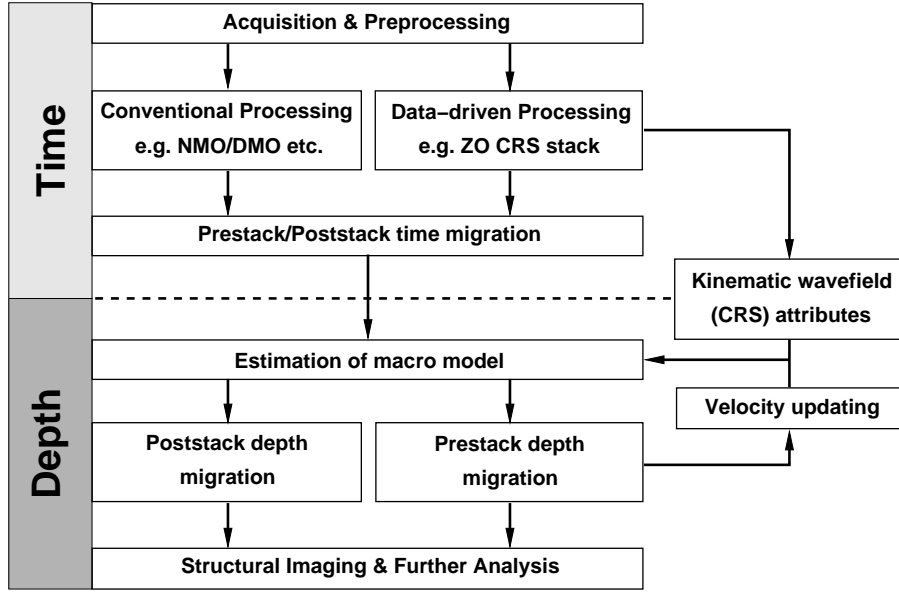


Figure 1: Integration of the Common-Reflection-Surface stack into the seismic reflection imaging workflow. [modified after Farmer et al. (1993)]

In this contribution, we present the basic concepts of a CRS-stack-based imaging strategy: starting with the preprocessed multicoverage data in the time domain, the CRS stack yields sufficient information for transforming these data into an image in the depth domain. We demonstrate the possibilities of this approach on a synthetic data example. An application to real data is shown by Heilmann et al. in this report.

For the synthetic example discussed here, a multi-coverage dataset was calculated by ray tracing in the blocky velocity model shown in Figure 2. The modeling of primary P-waves was performed using a marine acquisition geometry with a streamer of 2 km length, a source spacing of 25 m and a receiver group spacing of 12.5 m. The offset ranges from 250 m to 2250 m. A zero-phase Ricker wavelet with a dominant frequency of 30 Hz and a sampling interval of 4 ms was used. In addition, random noise was added to the data.

THE COMMON-REFLECTION-SURFACE (CRS) STACK

The simulation of stacked ZO sections is routinely applied to enhance the S/N ratio and to reduce the amount of seismic data for further processing. A conventional approach to achieve this goal is the application of normal-moveout (NMO) and dip-moveout (DMO) corrections to the multicoverage dataset followed by a subsequent stack along the offset axis, usually denoted as NMO/DMO/stack. The CRS stack is a powerful alternative to this conventional approach that can be seen as a generalized multi-dimensional high-density stacking-velocity analysis tool. It produces a simulated ZO section from the multicoverage data in a purely data-driven way. In addition, the CRS method provides a number of kinematic wavefield attributes associated with each ZO sample to be simulated. These attributes locally describe the shape of reflection events in the data. In the 2D case, the CRS stack fits entire stacking *surfaces* to the events rather than only stacking *trajectories*, as is done in conventional ZO simulation methods. Thus, far more traces contribute to each ZO sample, resulting in a higher S/N ratio, even for data of poor quality. The 2D stacking operator for a ZO sample (t_0, x_0) reads

$$t^2(x_m, h) = \left[t_0 + \frac{2 \sin \alpha (x_m - x_0)}{v_0} \right]^2 + \frac{2 t_0 \cos^2 \alpha}{v_0} \left[\frac{(x_m - x_0)^2}{R_N} + \frac{h^2}{R_{NIP}} \right], \quad (1)$$

where the half-offset h and the midpoint x_m between source and receiver describe the acquisition geometry and v_0 is the near-surface velocity assumed to be locally constant. The remaining three parameters are

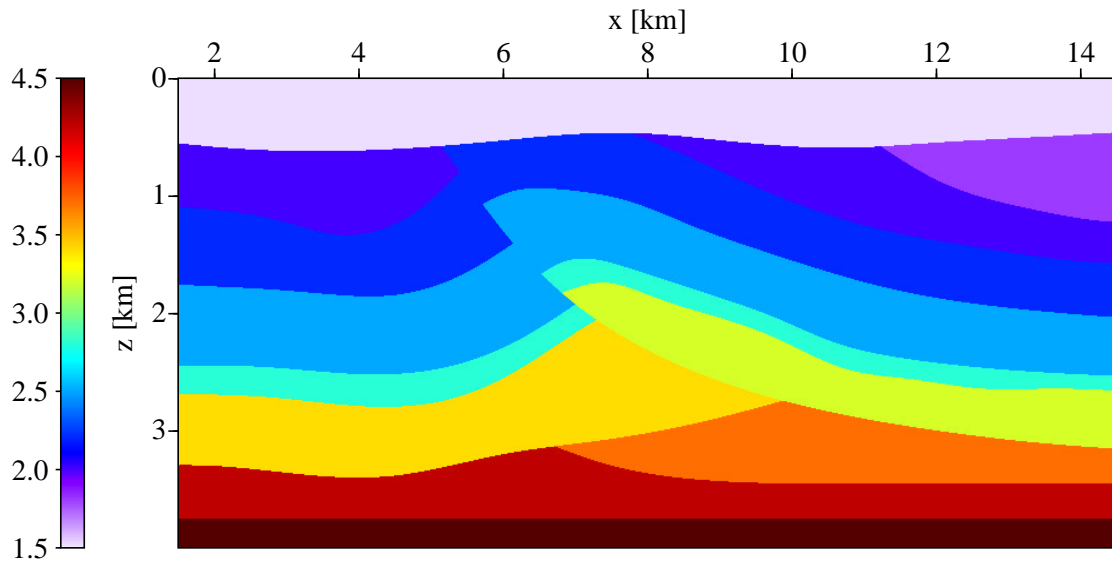


Figure 2: Blocky subsurface model used to calculate the synthetic multicoverage data. Shown is the P-wave velocity in km/s.

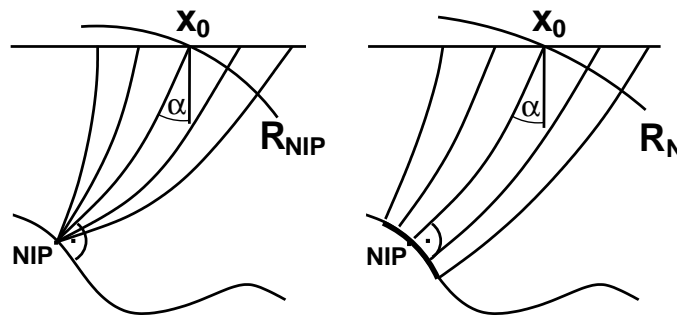


Figure 3: Hypothetical NIP wave (left) and normal wave (right) experiments. The angle α describes the emergence direction of the two hypothetical waves at the surface location x_0 . The parameters R_{NIP} and R_N are the observed radii of wavefront curvature associated with these waves.

the kinematic wavefield attributes. They describe the propagation direction (α) and radii of wavefront curvature (R_{NIP} , R_N) associated with two hypothetical experiments observed at $(z = 0, x_m)$. The NIP (normal incidence point) wave is the hypothetical wave that would be obtained by placing a point source at the NIP of the ZO ray. The N (normal) wave is the hypothetical wave that would be obtained by placing a small exploding reflector element at the NIP of the ZO ray. These hypothetical experiments are illustrated in Figure 3.

To determine the attributes of the CRS operator fitting best an actual reflection event, a coherence analysis is performed along stacking operators in the multicoverage data with different sets of kinematic wavefield attributes. At the locations of actual reflection events, the coherence values are influenced by the signal strength relative to the random noise along the events, by the number of contributing traces, and by the fit of the CRS operator to the actual events. The best fitting operator at a particular ZO location is expected to yield the highest coherence. This analysis is repeated for each ZO sample to be simulated, irrespective of whether there is an actual reflection event. In case of conflicting dip situations, also local coherence maxima have to be considered. Based on coherence analysis, the entire CRS approach can be applied in a noninteractive way and without the need for any a priori knowledge of a macrovelocity model.

The CRS stack was applied to the above-mentioned synthetic data. For the sake of simplicity, conflicting dip situations have not been considered in this example. The determination of the optimum stacking

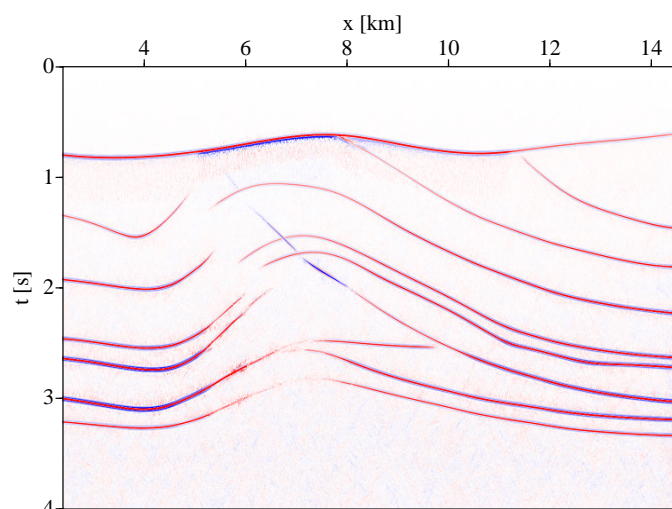


Figure 4: Simulated ZO section by means of the CRS stack.

operators and their associated wavefield attributes has been performed in separate steps with one search parameter each. This pragmatic approach of using certain subsets of the prestack data was introduced by Müller (1998). As this approach fails for a few ZO locations, a smoothing algorithm has been applied to the attribute sections which uses a combination of a median filter and averaging. Coherence and local dip of the reflection events are taken into account during smoothing, making it an event-consistent process. From a theoretical point of view, the smoothing is justified as the wavefield attributes can only vary smoothly along the reflection event and are virtually constant in the time direction along the seismic wavelet (Mann and Höcht, 2003). Details about this smoothing technique are given by Mann and Duvencek in this report. The smoothed attribute sections served as input to a local three-parameter optimization using the full spatial stacking operator (1) and the entire prestack data which yields the final wavefield attributes for stacking.

The simulated ZO section is displayed in Figure 4. The stacking aperture takes the projected ZO Fresnel zone into account which has been estimated from the wavefield attributes. The section containing the obtained coherence values along the stacking operators is displayed in Figure 5(d) together with the wavefield attribute sections: the emergence angle (Figure 5(a)) is clearly related to the dip of the reflection events, whereas the curvature of the normal wavefront (Figure 5(c)) is related to the curvature of the reflection events in the zero-offset section. This relationship is obvious: we observe positive values at convex parts of reflection events, negative values at concave parts of reflection events, and values close to zero when the reflection event's curvature goes to zero. Finally, the radius of curvature of the NIP wavefront is shown in Figure 5(b). In a constant velocity medium, this radius of curvature would coincide with the length of the normal ray (i. e., the distance to the NIP).

ATTRIBUTE-BASED TIME MIGRATION

Conventional time migration is based on a root-mean-square (RMS) velocity model in the time domain. In Kirchhoff migration, for a given location in the time-migrated domain, the diffraction response is calculated assuming a constant velocity model defined by the RMS velocity at the considered location. Summation of amplitudes along this surface yields the migration result which is assigned to the corresponding image point, i. e., the apex of the diffraction response. By repeating this step for all locations in the target zone, the entire time-migrated section is obtained. With the CRS wavefield attributes, that process can be performed in an approximate manner without the need for an explicit RMS velocity model (Mann et al., 2000).

The basic idea of the CRS-stack-based approach is quite simple: as mentioned above, the CRS stacking operator (1) provides an approximation of the kinematic reflection response in the time domain of a reflector segment in depth. It can be observed that in the case of a point diffractor the NIP and normal wave experiments as shown in Figure 3 coincide. If we gradually increase the curvature of the reflector in depth,

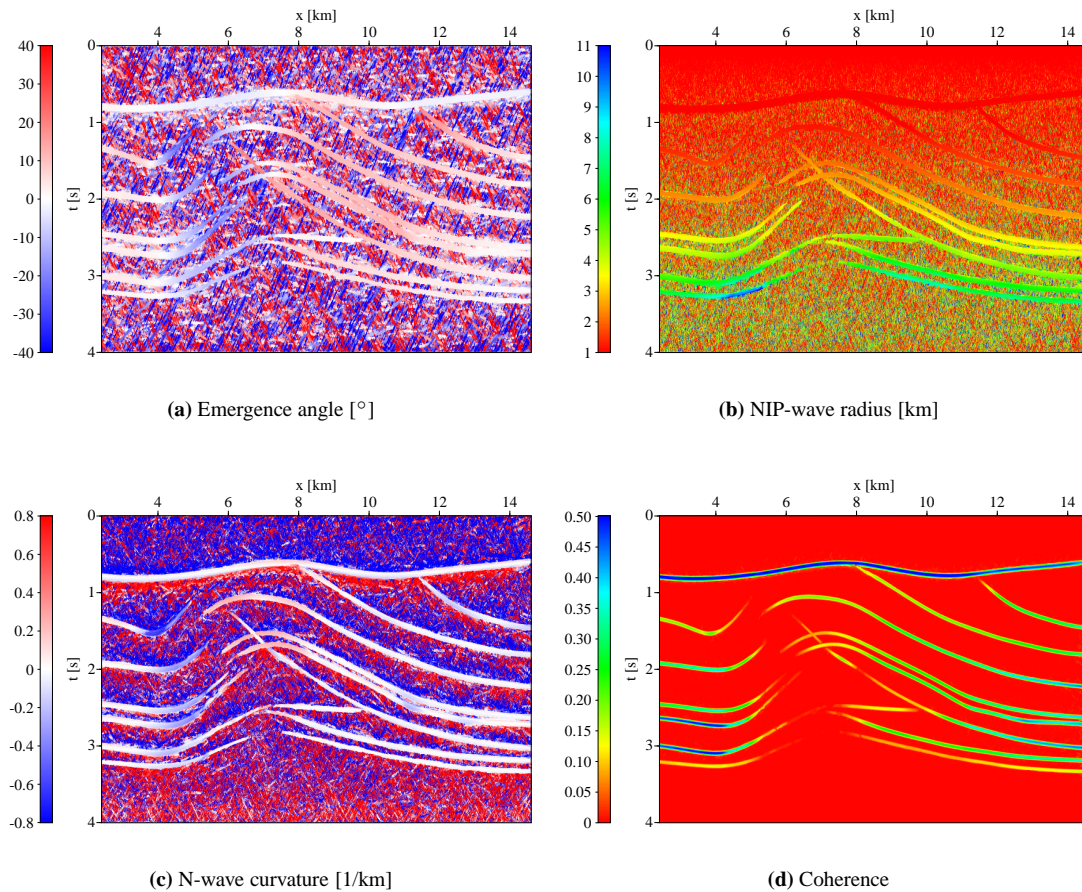


Figure 5: Kinematic wavefield attribute sections (a)-(c) and coherence section (d) obtained by the CRS stack method. The radius of curvature R_N is displayed as its inverse, i. e., the curvature of the normal wavefront. The coherence section has been clipped to a maximum of 0.5 to reveal weaker events. Note that the wavefield attributes are only meaningful along detected reflection events associated with sufficiently high coherence values.

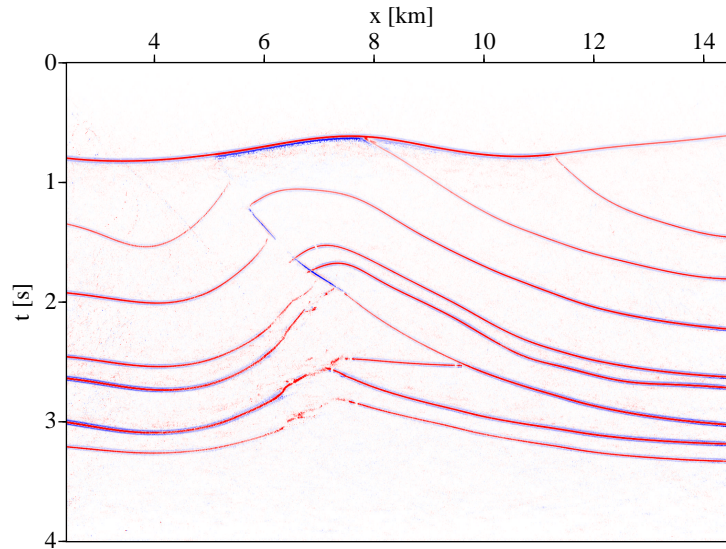


Figure 6: Attribute-based automated time migration result obtained as a by-product of the CRS stack. No RMS velocity model is needed and no actual diffraction stack has to be performed.

R_{NIP} remains unchanged whereas R_{N} converges to R_{NIP} . Thus, by setting $R_{\text{N}} := R_{\text{NIP}}$ in equation (1), we can approximate the response of a (hypothetical) diffractor at the NIP. Note that the actual subsurface location of the NIP is unknown whereas the kinematic wavefield attributes describing the NIP and normal wave have been extracted from the seismic data by means of the CRS stack. Thus, the required parameters to describe the approximate diffraction response are readily available for each ZO location. If we stack along this diffraction response and assign the result to its apex, a conventional time migration is approximated (for details, see Mann, 2002). In practice, instead of actually performing the stack along the diffraction response, we can make direct use of the already available CRS stack results: the CRS operator (1) fits closer to the actual reflection event than a diffraction response. This leads to a heuristic time migration which reduces to a mapping of the stack values to the apex of the approximate time migration operator. This can be performed very efficiently during the CRS stack by assigning the stack result not only to the ZO sample under consideration, but also to the approximate image location in the time-migrated section.

Figure 6 shows the result of this heuristic attribute-based time migration. Without any explicit RMS velocity model or actual summation along the diffraction responses, we obtain a structural image of the subsurface which may be used for a first interpretation of the data. This result can be obtained fully automatically as a by-product of the CRS stack with virtually no additional effort.

VELOCITY MODEL DETERMINATION AND MIGRATION

The estimation of a velocity model is one of the crucial steps in seismic depth imaging. Usually, the model is constructed iteratively, starting with an initial model and updating it by repeated prestack migration and analysis of residual moveouts in common-image gathers (CIGs). This is an expensive and time-consuming process. Approaches based on reflection tomography have the additional drawback of requiring extensive and often difficult picking in the prestack data.

The CRS technique offers an alternative which overcomes some of the drawbacks of conventional methods; the attributes R_{NIP} and α related to the NIP wave (Figure 3) at a given ZO location (x_0, t_0) describe the approximate multi-offset reflection response of a common reflection point (CRP) in the subsurface. Therefore, in a correct model, the NIP wave focuses at zero traveltimes at the NIP, when propagated into the subsurface. This principle can be utilized in an inversion that uses the attributes R_{NIP} and α picked in the CRS-stacked section to obtain a laterally inhomogeneous velocity model for depth imaging. The CRS-stack-based velocity determination approach is realized as a tomographic inversion, in which the misfit between picked and forward-modeled attributes is iteratively minimized in the least-squares sense. The

velocity model is defined by B-splines, i. e., a smooth model without discontinuities is used, which is well suited for ray-tracing applications.

As the attributes associated with each ZO sample already represent the multi-offset reflection response of a CRP, picking only has to be performed in the CRS-stacked ZO section. The picking procedure is further simplified due to the increased S/N ratio of the stacked section and may be automated based on the coherence section (Figure 5(d)). Because of the smooth model description, pick locations do not need to follow reflection events over consecutive traces.

The approximate description of the multi-offset CRP response with CRS attributes, however, leads to a limitation of the allowed degree of lateral inhomogeneity in the model. Furthermore, a smooth model description may be inappropriate in some cases (e. g., salt bodies of complicated shape). Details of the method are described in Duveneck (2004) and in the WIT report 2002.

The tomographic inversion based on CRS attributes was applied to the synthetic data example introduced above. About 700 data points have been automatically picked in the coherence section, Figure 5(d). The corresponding attributes have been simultaneously extracted from the R_{NIP} and α sections, Figures 5(b) and 5(a). These data entered into the inversion algorithm. The inversion result consists of the reconstructed velocity model and the reconstructed normal rays associated with the picks. Figure 7(a) shows the velocity model together with the endpoints of the normal rays, i. e., the reconstructed NIPs. In Figure 7(b), the latter are superimposed on the true blocky velocity model for comparison.

With the obtained velocity model, a Kirchhoff prestack depth migration and a poststack depth migration of the CRS stack result (Figure 4) have been performed. The poststack migration result is depicted in Figure 8(a). Due to poor illumination, the lowermost horizontal reflector is incompletely imaged below the complex part of the model. This problem is partly resolved by the application of prestack depth migration. As can be seen in Figure 8(b), the lowermost reflector is here more continuous, although it could not be exactly positioned in depth everywhere. A selection of CIGs (every 1000 m) is displayed in Figure 9. Almost all events in the CIGs are flat, which implies that the reconstructed velocity model is kinematically consistent with the data. This even applies for the partly incorrectly positioned lowermost reflector, indicating that the solution of the inversion is not unique.

CONCLUSIONS

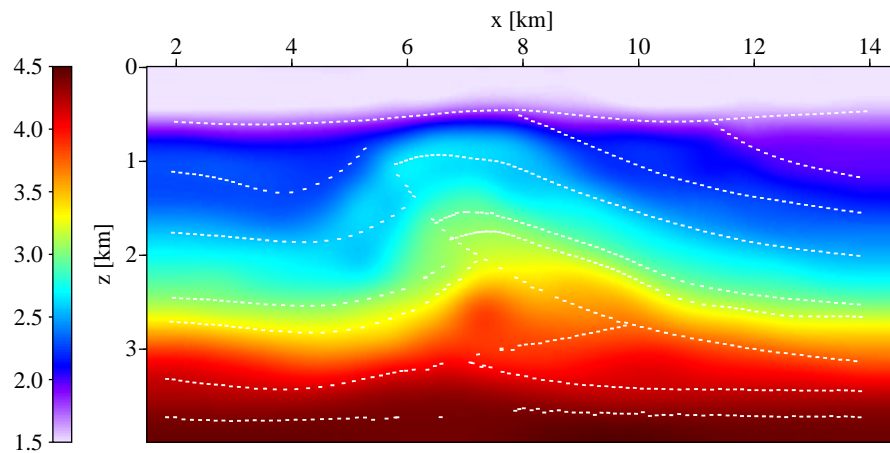
We have demonstrated that the CRS stack and the associated kinematic wavefield attributes can be used in seismic imaging applications which go far beyond the purposes for which the method was originally designed—the simulation of ZO sections with improved S/N ratio. The kinematic wavefield attributes can be used to perform an approximate automated time migration. In addition, they contain information that can be used for the estimation of velocity models for depth migration. Apart from the applications discussed here, the CRS stack has potential in other seismic processing topics such as static corrections or redatuming. In particular, data of poor quality or data with irregular acquisition geometries are expected to benefit from this approach.

ACKNOWLEDGMENT

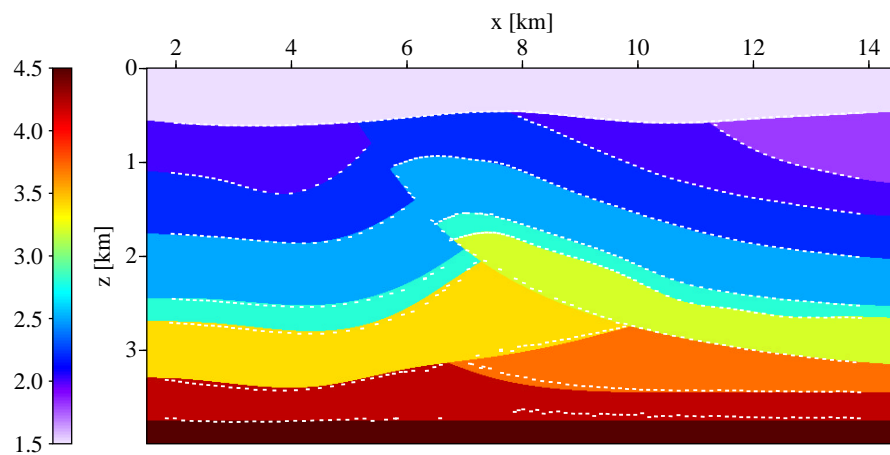
The authors would like to thank the sponsors of the *Wave Inversion Technology (WIT)* Consortium for their support.

REFERENCES

- Duveneck, E. (2004). Velocity model estimation with data-derived wavefront attributes. *Geophysics*, 69(1). In print.
- Duveneck, E. and Hubral, P. (2002). Tomographic velocity model inversion using kinematic wavefield attributes. In *Expanded Abstracts. 72nd Ann. Internat. Mtg., Soc. Expl. Geophys. Session IT 2.3*.
- Farmer, P., Gray, S., Hodgkiss, G., Pieprzak, A., Ratcliff, D., and Whitcombe, D. (1993). Structural Imaging: Toward a Sharper Subsurface View. *Oilfield Review*, 5:28–41.
- Hubral, P., editor (1999). *Macro-model independent seismic reflection imaging*. J. Appl. Geophys., 42(3,4).

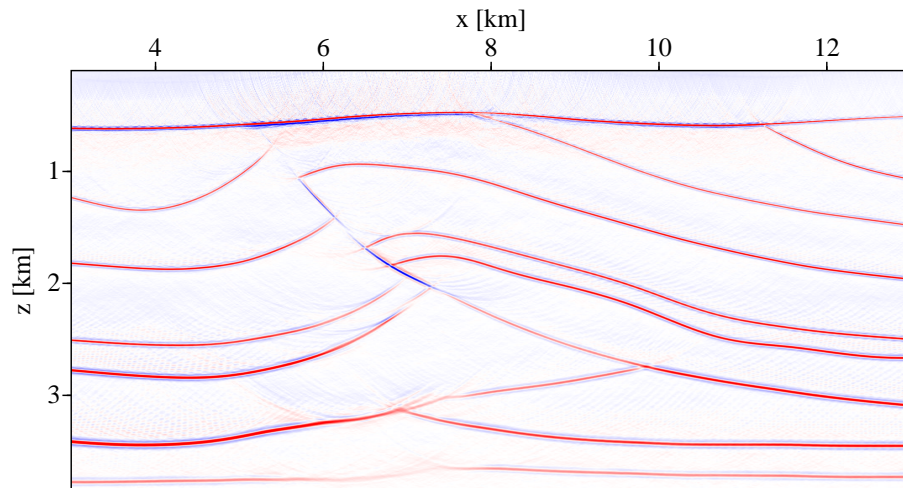


(a) Reconstructed P-wave velocity model [km/s]

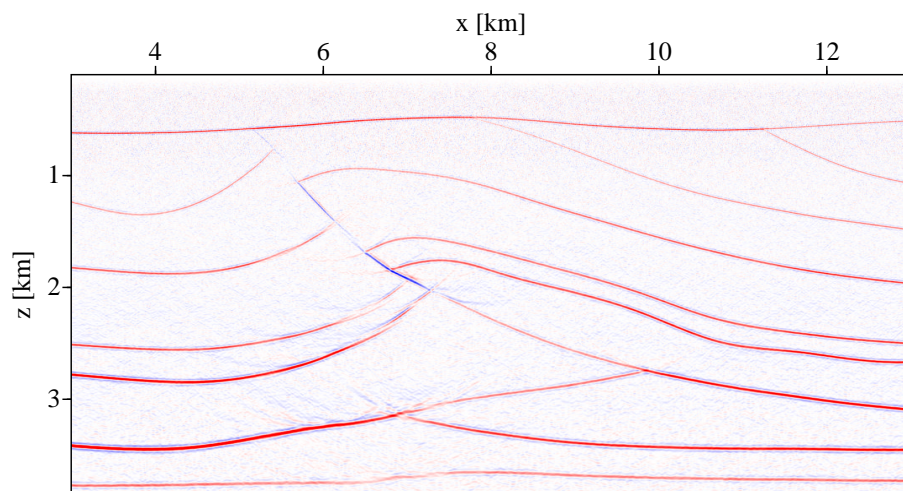


(b) True P-wave velocity model [km/s]

Figure 7: Reconstructed and true P-wave velocity models with reconstructed reflector points (white dots) superimposed. Each depicted reflector point corresponds to a data point which has automatically been picked in the CRS stack results.



(a) Poststack-migrated section of the CRS stack result (Figure 4).



(b) Stack of prestack-migrated common-offset sections.

Figure 8: Comparison of poststack and prestack depth migration results obtained with the reconstructed smooth velocity model (Figure 7(a)).

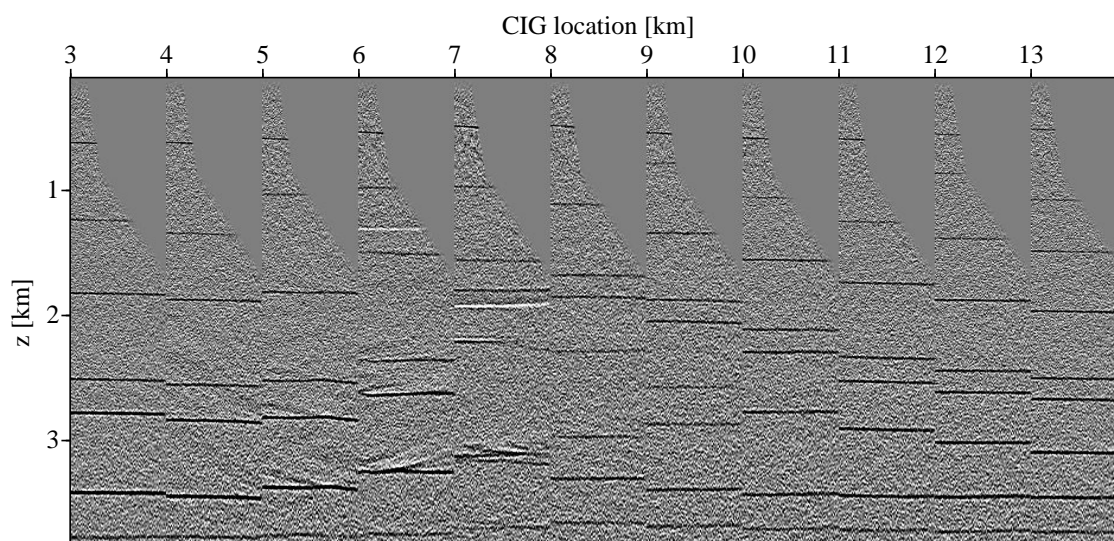


Figure 9: A set of CIGs extracted from the prestack-migrated common-offset sections obtained with the reconstructed smooth velocity model (Figure 7(a)). For each CIG, the offset ranges from 0.25 to 2.25 km. Almost all events are flat.

Jäger, R., Mann, J., Höcht, G., and Hubral, P. (2001). Common-Reflection-Surface stack: Image and attributes. *Geophysics*, 66:97–109.

Mann, J. (2002). *Extensions and Applications of the Common-Reflection-Surface Stack Method*. Logos Verlag, Berlin.

Mann, J. and Höcht, G. (2003). Pulse stretch effects in the context of data-driven imaging methods. In *Extended Abstracts*. 65th Ann. Internat. Mtg., Eur. Assn. Geosci. Eng. Session P007.

Mann, J., Hubral, P., Traub, B., Gerst, A., and Meyer, H. (2000). Macro-Model Independent Approximative Prestack Time Migration. In *Extended Abstracts*. 62nd Ann. Internat. Mtg., Eur. Assn. Geosci. Eng. Session B-52.

Müller, T. (1998). Common Reflection Surface Stack versus NMO/STACK and NMO/DMO/STACK. In *Extended Abstracts*. 60th Ann. Internat. Mtg., Eur. Assn. Geosci. Eng. Session 1-20.

Müller, T. (1999). *The Common Reflection Surface Stack Method – Seismic imaging without explicit knowledge of the velocity model*. Der Andere Verlag, Bad Iburg.

Vieth, K.-U. (2001). *Kinematic wavefield attributes in seismic imaging*. PhD thesis, University of Karlsruhe.

Yilmaz, Ö. (2001). *Seismic Data Analysis*. Soc. Expl. Geophys., Tulsa.